NIH Public Access
Author Manuscript
Organometallics. Author manuscript; available in PMC 2014 May 24.

Published in final edited form as:
Organometallics. 2013 May 24; 32(10): 3053–3062. doi:10.1021/om400281v.

Heterolytic H_2 Cleavage and Catalytic Hydrogenation by an Iron Metallaboratrane

Henry Fong, **Marc-Etienne Moret**[†], **Yunho Lee**[‡], and **Jonas C. Peters**[*]
Division of Chemistry and Chemical Engineering, California Institute of Technology, Pasadena, CA 91125, USA

Abstract

Reversible, heterolytic addition of H_2 across an iron-boron bond in a ferraboratrane with formal hydride transfer to the boron gives iron-borohydrido-hydride complexes. These compounds catalyze the hydrogenation of alkenes and alkynes to the respective alkanes. Notably, the boron is capable of acting as a shuttle for hydride transfer to substrates. The results are interesting in the context of heterolytic substrate addition across metal-boron bonds in metallaboratranes and related systems, as well as metal-ligand bifunctional catalysis.

Keywords

Metallaboratrane; non-noble metal hydrogenation catalysis; heterolytic dihydrogen activation

INTRODUCTION

Transition metal-catalyzed bond forming reactions often involve formal two-electron redox steps (e.g., oxidative addition and reductive elimination). Noble metal catalysts are commonly used in these reactions due, in part, to their propensity to facilitate multi-electron processes.[1] There is growing interest in developing catalysts for bond forming/cleavage reactions based on earth abundant mid-to-late first-row transition metals, a goal that presents a unique set of challenges.[2] First-row transition metal catalysts that can circumvent undesirable one electron processes in favor of concerted two electron reaction steps present one plausible design criterion.[3]

Cooperative catalysis strategies that utilize ligands that operate in tandem with a coordinated metal center to activate substrates have shown promise in addressing this issue.[4,5] First-row metallaboratranes and related compounds that contain a retrodative M→B σ-interaction[6] are appealing as catalysts[7] because of the boron center's ability to stabilize low valent metals.[8] Akin to frustrated Lewis pairs,[9] it has also been recently demonstrated that the metal-boron interaction can cooperatively facilitate the activation of H_2.[5,7] For instance, our lab recently reported that the diphosphine-borane nickel (^{Mes}DPB^{Ph})Ni complex undergoes reversible oxidative addition of H_2 to afford a nickel-borohydrido-hydride complex (Scheme 1).[10] This

[*]Corresponding Author: jpeters@caltech.edu.
[†]Organic Chemistry and Catalysis Group, Faculty of Science, Utrecht, Universiteitsweg 99, 3584 CG Utrecht, The Netherlands; m.moret@uu.nl
[‡]Department of Chemistry, School of Molecular Science, Korea Advanced Institute of Technology, 291 Daehak-ro Yuseong-gu, Daejeon 305-701, Republic of Korea; yunholee@kaist.ac.kr

The authors declare no competing financial interests.

Supporting Information. Spectral data, catalysis data, computational details, solid state structures (**4** and **(SiP^{iPr}$_3$)Fe(CO)(H)**), and CIF files (for **2**, **3**, **4**, **5**, **8**, **10**, **11**, and **(SiP^{iPr}$_3$)Fe(CO)(H)**). This material is available free of charge via the Internet at http://pubs.acs.org.

NIH-PA Author Manuscript
NIH-PA Author Manuscript
NIH-PA Author Manuscript

NIH-PA Author Manuscript

NIH-PA Author Manuscript

NIH-PA Author Manuscript

nickel system is an efficient catalyst for olefin hydrogenation. Kameo and Nakazawa have also reported on the transfer hydrogenation of ketones catalyzed by a rhodium diphosphine-borane complex.[11]

Herein we report on studies of heterolytic H-H bond cleavage at a ferraboratrane complex[12] of a triphosphine-borane (TPB) ligand.[13] Dihydrogen is shown to add reversibly across the Fe-B bond of (TPB)Fe(L) complexes to form corresponding iron-borohydrido-hydride complexes of the type (TPB)(μ-H)Fe(L)(H). Like the nickel system reported previously, olefin hydrogenation catalysis is accessible, albeit much slower, thereby facilitating detailed studies. As discussed below, other E-H bonds are also activated by the ferraboratanes described, including the terminal C-H bonds of arylacetylenes and the C-H bonds of formaldehyde.

RESULTS AND DISCUSSION

Reversible H_2 Addition

Exposing the previously reported (TPB)Fe(N_2) complex[12a] (**1**) in d_6-benzene to H_2 (1.2 equiv) at room temperature results in H_2 addition across the Fe-B bond to give a yellow solution of the six coordinate borohydride-hydride-N_2 complex (TPB)(μ-H)Fe(N_2)(H) (**2**) (Scheme 2, Figure 1). The XRD structure of **2** shows that the Fe-B distance is significantly elongated relative to **1** (2.604(3) Å in **2** versus the calculated distance of 2.2 Å in **1**[12b]) (Figure 1). A terminal hydride ligand and a bridging hydride ligand located between the B and Fe atoms can be assigned from the electron density difference map. This structure also prevails in solution. In the ^{1}H NMR spectrum (d_6-benzene), the terminal hydride ligand on iron is observed as a triplet-of-doublets at −9.6 ppm, and the bridging hydride is observed as a broad singlet at −30.4 ppm. Replacing H_2 with D_2 in the reaction gives the corresponding isotopologue (TPB)(μ-D)Fe(N_2)(D). Along with the expected deuteride signals in the ^{2}H NMR spectrum, deuterium signals from the methine and terminal methyl positions of the isopropyl groups of the TPB ligand are observed. This observation establishes that facile scrambling of the hydridic ligands into the TPB isopropyl groups occurs, presumably via a reversible C-H metalation process.

The dinitrogen ligand (ν_{NN} = 2070 cm^{-1}) in **2** is labile, and it can be substituted under excess H_2 to give the dihydrogen analogue (TPB)(μ-H)Fe(H_2)(H) (**3**) (Scheme 2). Exposing **1** to excess H_2 (1 atm) also generates **3**. Its XRD structure again confirms the presence of a bridging hydride (Figure 2). Although electron density can be located in the difference map between a widened P-Fe-P angle (136.54(2)°) and in the apical position *trans* to the borohydride unit, the data do not allow us to reliably distinguish between classical and non-classical hydrides. We therefore turned to NMR spectroscopy to aid in the formulation of **3**.

The 20 °C ^{1}H NMR spectrum (d_8-toluene) of **3** (Figure 3) shows a broad singlet resonance at −15.1 ppm, indicative of hydridic protons. A broad deuteride signal is observed in the ^{2}H NMR spectrum when D_2 is used in place of H_2, and, like in **2**, deuterium signals are also observed in the methyl and methine positions of the isopropyl groups of the TPB ligand. Cooling a d_8-toluene solution of **3** under an H_2 atmosphere to −20 °C leads to sharpening of the resonance at −15.1 ppm, which integrates to three protons (3H). A second, broad hydridic resonance integrating to one proton is also observed at −24.9 ppm, and in analogy to **2**, this resonance is assigned to the bridging-borohydride (μ-H). Cooling down to −90 °C leads to broadening of the 3H resonance without reaching decoalescence, suggesting that exchange of three hydrogenic ligands is fast on the NMR timescale. Compound **3** can be heated to 50 °C before significant sample decomposition is observed (*vide infra*). At 50 °C, the 3H and μ-H signals both broaden into the baseline, suggesting that exchange of all four hydrogens is facile at this temperature.

NIH-PA Author Manuscript

NIH-PA Author Manuscript

NIH-PA Author Manuscript

To further assign the 3H unit in **3** (i.e. dihydrogen-hydride versus trihydride), we turned to minimal longitudinal relaxation (T_{1min}) measurements.[14,15] The T_{1min} is 35 ms at −32 °C for the 3H resonance, which suggests that the 3H unit is best described as dihydrogen-hydride and implying the following assignment for **3**: (TPB)(μ-H)Fe(H_2)(H). This interpretation is additionally supported by DFT calculations (RB3LYP/6-31G(d)) that identify a dihydrogen-hydride structure (Figure 2 and Supporting Information) as the lowest energy isomer of **3**. A stereoisomer in which the H_2 ligand occupies the equatorial position and the hydride ligand is in the axial position *trans* to boron is calculated to be 6.1 kcal/mol higher in energy. This geometric preference parallels that of the well-characterized iron-dihydrogen-dihydride complex *mer*-Fe(H_2)(H)$_2$(PEt$_2$Ph)$_3$.[16] The transition state for conversion of **3** into this higher energy stereoisomer involving H-H scission is calculated to be 6.7 kcal/mol above the most stable isomer and is in line with the observed exchange behavior on the NMR timescale.

Analogous (TPB)(μ-H)Fe(L)(H) complexes (L = CN^{t}Bu (**5**), CO (**7**)) can be synthesized (Scheme 2, Figure 1). To explore the effect of the apical ligand L on the H-H bond activation process, (TPB)Fe(L) complexes (L = CN^{t}Bu, **4**; L = CO, **6**) were prepared. The previously reported carbonyl complex **6** displays an η^3-interaction with a P-C$_{Ar}$-C$_{Ar}$ unit of the TPB ligand[12a] whereas isocyanide adduct **4**, whose structure has been determined, does not: its Fe center is rigorously 5-coordinate. Complex **6** is diamagnetic whereas **4** gives rise to a solution magnetic susceptibility (μ_{eff} = 1.7 μ_B) at room temperature in C_6D_6. The temperature dependence of the solution susceptibility suggests an S = 0 ground state with a thermally accessible S = 1 state. No reaction occurs between (TPB)Fe(CN^{t}Bu) (**4**, μ_{eff} = 1.7 μ_B) or the previously reported (TPB)Fe(CO)[12a] (**6**) with H_2 (1 atm) at room temperature over a period hours. Compound **4** is fully consumed by H_2 (1 atm) over the course of 3 days at 40 °C to generate **5**, while compound **6** is fully consumed by H_2 (1 atm) over the course of 5 days at 80 °C to give **7**. The increase in temperature and reaction time compared to the facile room temperature reaction between **1** and H_2 is consistent with a scenario in which H_2 substitution for L occurs prior to H_2 addition across the Fe-B bond. Complex **7** can be alternatively synthesized from **1** or **2** and formaldehyde (Scheme 2).

Dihydrogen addition across the Fe-B bond of **1** is reversible. Conversion of **3** to **2** and subsequently back to **1** can be effected by exposing **3** to dynamic vacuum and then N_2, or by repeated freeze-pump-thaw-N_2 cycles. Reformation of the Fe-B bond can also occur through hydride transfer to unsaturated substrates (*vide infra*). Dihydrogen elimination from **5** and **7** does not occur when treated similarly.

Worth underscoring is that cleavage of the Fe-B bond in the present ferraboratrane system is distinct from the H_2 chemistry observed for a structurally related (SiP$^{i\mathrm{Pr}}_3$)Fe silatrane system (SiP$^{i\mathrm{Pr}}_3$= [Si(*o*-C$_6$H$_4$P$^{i\mathrm{Pr}}_2$)$_3$]$^-$,) we have introduced elsewhere.[17,18,19] For instance, the reaction between (SiP$^{i\mathrm{Pr}}_3$)Fe(N_2) and H_2 affords (SiP$^{i\mathrm{Pr}}_3$)Fe(H_2), and that between [(SiP$^{i\mathrm{Pr}}_3$)Fe(N_2)]$^+$ and H_2 affords [(SiP$^{i\mathrm{Pr}}_3$)Fe(H_2)]$^+$. No disruption of the Fe-Si bond is observed in either case, even if for instance isolated [(SiP$^{i\mathrm{Pr}}_3$)Fe(N_2)]$^+$ or [(SiP$^{i\mathrm{Pr}}_3$)Fe(H_2)]$^+$ is exposed to excess H_2. Ligand substitution instead occurs. This sharply contrasts isoelectronic (TPB)Fe(N_2) **1**, where H_2 addition readily affords the cleavage product **2** or **3**. We also find (this report, Scheme 3) that hydrogenolysis of the iron(II) methyl complex (SiP$^{i\mathrm{Pr}}_3$)Fe(Me) occurs slowly at 60 °C to give an H_2/H product, but once again without disruption of the Fe-Si bond. Addition of exogenous donor ligands such as H_2, N_2 and CO effects substitution of the coordinated H_2 ligand, but the Fe-Si bond is maintained. One factor contributing to the difference between the two systems is likely the more flexible Fe-B bond in the (TPB)Fe system, as reflected in the variable Fe-B bond distances (varying by *ca.* 0.5 Å)[12b] versus more rigid Fe-Si bond distances (varying by *ca.* 0.2 Å)[17,18,19] in (SiP$^{i\mathrm{Pr}}_3$)Fe that have been observed over several formal iron oxidation states. The rigidity of

NIH-PA Author Manuscript

NIH-PA Author Manuscript

NIH-PA Author Manuscript

the Fe-Si interaction presumably reflects an appreciably stronger Fe-Si bond relative to Fe-B. One can additionally consider the relative Lewis acidity of the Ar_3B versus the Ar_3Si^+ subunit[18] in these respective systems, and their propensity to serve as H^- acceptors, but one might then predict the Ar_3Si^+ to be the better acceptor, in contrast to the experimental observations. Indeed, this latter point may be the reason the Fe-Si interaction is stronger than the Fe-B interaction.

Reaction with Unsaturated Substrates

The ability of the (TPB)Fe scaffold to reversibly cleave H_2 prompted us to study if the transfer of hydrogen from (TPB)(μ-H)Fe(L)(H) to substrates is possible. The reaction of **1** with ethylene, styrene and arylacetylenes was probed. A degassed d_6-benzene solution of **1** reacts with ethylene to give a light brown solution of the paramagnetic iron-ethylene adduct (TPB)Fe(C_2H_4) (**8**; μ_{eff} = 3.2 μ_B, S = 1) (Scheme 4). Brown XRD quality crystals of **8** can be grown under an atmosphere of ethylene at 0 °C. Two molecules of **8** are found in the asymmetric unit cell. The iron center is bound η^2 to ethylene ($(Fe\text{-}C)_{avg}$ = 2.108(1) Å) and lies above the plane defined by the phosphine donors by an average distance of 0.641 Å, with a corresponding elongation of the average Fe-B distance to 2.491(2) Å (compared to 2.2 Å in **1**). The average C-C bond distance ($(C\text{-}C)_{avg}$ = 1.397(2) Å) of the η^2-coordinated ethylene molecule is significantly elongated from that in free ethylene (1.337 Å). [20] The data are consistent with π-backbonding from iron to ethylene, which confers significant ferracyclopropane character to **8**.[21] Storing **8** for two days under an atmosphere of N_2 fully regenerates **1**.

Compound **1** does not afford a detectable styrene adduct but reacts with both phenyl- and tolylacetylene with formal hydride transfer from the terminal C(sp)-H of the arylacetylene to the boron, forming S = 2 iron-borohydrido-arylacetylide complexes (TPBH)Fe(C_2Ar) (Ar = Ph, **9**, μ_{eff} = 5.1 μ_B; Ar = Tol, **10**, μ_{eff} = 5.2 μ_B) (Scheme 4). Two molecules of **10** are found in the asymmetric unit, and the XRD structure shows the presence of a tolylacetylide ligand coordinated to a pyramidalized iron center (Figure 4). While the hydride on the boron cannot be reliably located by XRD, the IR spectra for both **9** and **10** show B-H stretches at 2490 cm^{-1} and 2500 cm^{-1}, respectively, most consistent with a non-bridging B-H unit. The vibrational bands shift to 1826 cm^{-1} (predicted 1834 cm^{-1}) for **9** and 1824 cm^{-1} (predicted 1841 cm^{-1}) for **10** upon labeling with the monodeuterated arylacetylene (ArC≡CD).

The activation of the arylacetylene C(sp)-H bond by **1** is reversible. Mixing a d_6-benzene solution of **9** with tolylacetylene (4 equiv) and, conversely, mixing a d_6-benzene solution of **10** with phenylacetylene (4 equiv) both result in a mixture of **9** and **10** (Scheme 5A). The corresponding exchange reactions with B-D labelled isotopologues of **9** or **10** ((TPBD)Fe(C_2Ar)) and a different all-protio arylacetylene (Ar'C≡CH) result in the exclusive formation of free ArC≡CD, indicating that the arylacetylene unit is reductively eliminated from the iron-borohydrido-arylacetylide complexes prior to activation of an incoming acetylene substrate, presumably by reversible hydride transfer from the boron to the arylacetylide to form intermediate π-adducts akin to **8** (Scheme 5B).

Stoichiometric Hydrogenations

We also explored whether the transfer of hydrogen from (TPB)(μ-H)Fe(L)(H) species to unsaturated substrates might be possible. Exposing **8** to excess H_2 (1 atm) results in complete conversion of ethylene to ethane and **3** as the iron-containing product (Scheme 6-i) in less than 12 h. A paramagnetic intermediate (**A**) and **8** can be observed by *in situ* ^{1}H NMR spectroscopy. The same paramagnetic intermediate **A** and **8** can also be observed by *in situ* ^{1}H NMR spectroscopy if the same reaction is run under ethylene (1 atm) and H_2 (1 atm). The IR spectrum of the reaction mixture shows a diagnostic terminal B-H vibration at

NIH-PA Author Manuscript

NIH-PA Author Manuscript

NIH-PA Author Manuscript

2470 cm^{-1} that is attributed to **A**. Akin to the iron-borohydrido-alkynyl complexes **9** and **10**, **A** is assigned to the iron-borohydrido-ethyl complex (Scheme 6-i).[22] Using D_2 in place of H_2 in the ethylene hydrogenation reaction and monitoring leads to the observation of both B-D and B-H stretches in the IR spectrum, which is consistent with facile insertion/β-hydride elimination processes prior to ethane elimination from **A**. We note the similarity of **A** (and **9** and **10**) to the well-characterized zwitterionic, *tris*(phosphino)borate-iron-ethyl complex ($PhBP_3$)Fe(Et) that was observed as an intermediate in ethylene hydrogenation with the previously reported iron ($PhBP_3$)Fe system.[3e]

Complexes **1**, **2**, and **3** hydrogenate both phenylacetylene (1 equiv) and styrene (1 equiv) to ethylbenzene (1 atm H_2) with **3** as the observable iron-containing product. The *in situ* ^{1}H NMR spectrum of styrene hydrogenation reactions using **1**, **2**, or **3** show styrene, ethylbenzene and **3** in solution during the reaction course. Furthermore, for styrene hydrogenation with D_2 the ^{2}H NMR spectrum and GC-MS data of the reaction mixture show incorporation of deuterium onto both olefinic carbon atoms of free styrene, indicating that styrene coordination to the iron-center and insertion/β-hydride elimination processes are reversible.

Under stoichiometric conditions, the addition of 1 equiv of styrene to a solution of **2** in d_6-benzene and under N_2 (1 atm) cleanly generates 1 equiv of ethylbenzene and **1** (Scheme 6-ii). In contrast, running the same reaction under a static vacuum yields a mixture of styrene, ethylbenzene, **1**, and **2** (Scheme 6-iii). These observations suggest that excess H_2 or N_2 is required for the hydrogenations to proceed to completion. Moreover, the bridging monohydride appears competent for transfer to a substrate.

Substrates including *trans*-stilbene, N-benzylideneaniline, acetone, and acetophenone were not hydrogenated under similar conditions. Compounds **5** and **7** also do not hydrogenate ethylene, styrene, or phenylacetylene under the same conditions.

Catalytic Hydrogenations

Under the catalytic conditions of 0.01 M **1**, 1 atm of H_2, and 30 equiv of the substrate in d_6-benzene at room temperature, ethylene, styrene, and phenylacetylene are hydrogenated to ethane and ethylbenzene, respectively (Table 1). Compounds **2** and **3** can also be used as precatalysts. Ambient laboratory light does not affect the reaction and the catalysis is not inhibited by elemental mercury; it thus appears to be a homogeneous process. Norbornene is hydrogenated to norbornane, and with an atmosphere of D_2 in place of H_2 the *cis*-addition product *exo,exo*-2,3-d_2-norbornane[23] is exclusively observed, indicating the syn-addition of hydrogen and arguing against radical processes.

The hydrogenation catalysis was monitored by ^{1}H NMR spectroscopy with ferrocene as an internal integration standard. As with stoichiometric ethylene hydrogenation, the *in situ* ^{1}H NMR spectra of the catalytic ethylene hydrogenation reaction indicate the presence of ethylene adduct **8** and the putative ethyl-borohydride intermediate **A** as the iron-containing species during the reaction course. Complex **3** is the iron-containing product at the completion of the reaction. For styrene hydrogenation, styrene, ethylbenzene, and **3** are observed during catalysis, and scrambling of deuterium into the vinylic positions of styrene is observed under D_2. In contrast, for phenylacetylene hydrogenation complex **9** is the only observed iron-species early in the reaction when the phenylacetylene concentration is high. As phenylacetylene is consumed, styrene and **3** form, and ethylbenzene begins to develop slowly thereafter.

Attempting to increase the rate of catalysis by elevating the reaction temperature results in catalyst decomposition. The decomposition product (**11**) can be synthesized independently

NIH-PA Author Manuscript

NIH-PA Author Manuscript

NIH-PA Author Manuscript

in near quantitative yields by heating **3** (80 °C) under H_2 (1 atm) for 2 h. The XRD structure of **11** indicates that a B-C_{Ar} bond is cleaved from the TPB ligand fragment (Figure 5). This result offers the cautionary note that B-C_{Ar} bond cleavage to give metal-borohydride products is a viable catalyst decomposition pathway.

Based on the results from the stoichiometric and catalytic experiments, we propose a plausible mechanistic scenario to account for the observed catalytic styrene hydrogenation by **1** (Scheme 7A), and in doing so underscore interesting aspects of the mechanism that remain unanswered. Starting from precatalyst **1**, addition of H_2 generates **3**, a species that can be observed by ^{1}H NMR spectroscopy during catalytic runs (resting state). Subsequent substitution of the apical H_2 ligand for styrene forms the unobserved iron-styrene-hydride-borohydride species **B**, and insertion into the terminal hydride affords the iron-alkyl intermediate **A′**. Intermediate **A′** is analogous to the ethyl species **A** (Scheme 6-i), and is also related to the structurally characterized acetylide-borohydride complex **10** (Scheme 4). Olefin coordination and insertion appears to be reversible, as labeling studies show deuterium is exchanged into the vinylic positions of *free* styrene under a D_2 atmosphere. Elimination of ethylbenzene in the presence of H_2 regenerates the catalyst resting state.

The conversion of **1** to **3** likely proceeds via the H_2-adduct intermediate **C** depicted in Scheme 7B by H_2-for-N_2 ligand exchange. While we have not detected such a species in the present (TPB)Fe system, its cobalt analogue (TPB)Co(H_2) can be isolated and has been thoroughly characterized,[24] as has the isoelectronic iron complex $[(SiP^{i}Pr_3)Fe(H_2)]^{+}$.[17] N_2/H_2 exchange is facile in these well-defined Co and Fe systems, and by extension we infer it would also be facile for (TPB)Fe(N_2) **1** to afford (TPB)Fe(H_2) **C** before additional reactions ensue. Since H_2 reacts with **1**, but not with **5** and **7** at room temperature, we think that facile H_2 substitution for N_2 most likely occurs prior to H-H bond cleavage. We appreciate that while this scenario is consistent with the data available, it is not demanded by the available data. For instance, it is alternatively possible that styrene substitution for the N_2 ligand in **1** precedes H_2 addition to form intermediate **B**. No direct evidence rules out this possibility. We prefer suggesting that the H_2/dihydride species **3** precedes styrene binding because of the observation that H_2 addition/activation by other (TPB)Fe(L) adducts, for example **4** and **6**, is very slow, and also because N_2, and presumably therefore also H_2, displaces ethylene from **8** in solution (regenerating **1** or (TPB)Fe(H_2)).

The final ethylbenzene elimination step can be envisioned to occur through two plausible routes (Scheme 7B). One such pathway involves a reductive elimination step where hydride transfer directly from the borohydride subunit generates the alkane product to form **3**, likely via the dihydrogen adduct intermediate **C**. The other pathway proceeds through alkane elimination by hydrogenolysis of the phenylethyl group without hydride transfer from the borohydride subunit.

While the available data do not firmly distinguish between the two product elimination pathways shown in Scheme 7B, the stoichiometric hydrogenation studies described above show that 1 equiv of styrene is completely hydrogenated to ethylbenzene by **2** under an N_2 atm (Scheme 6-ii). This observation implies that **2** can serve as the source of the two H-atom equivalents delivered to styrene. From complex **2**, substitution of the apical N_2 ligand for styrene in **2** would generate the styrene adduct intermediate **B**. Subsequent insertion of the bound styrene into the *cis* Fe-H would afford intermediate **A′**, which in the absence of H_2 at least, eliminates ethylbenzene concomitant with N_2 binding to reform **1**. The presence of exogenous N_2 (or alternatively H_2) facilitates the generation of ethylbenzene. As noted in Scheme 6-iii, the stoichiometric reaction under static vacuum between **2** and styrene is quite slow compared with the same reaction under N_2 (Scheme 6-ii). This observation can be

NIH-PA Author Manuscript

NIH-PA Author Manuscript

NIH-PA Author Manuscript

explained by presuming the conversion of intermediate **A′** to **1** requires N_2 association prior to elimination to generate ethylbenzene.

CONCLUSIONS

In summary, we have demonstrated that the Fe-B bond in ferraboratranes (TPB)Fe(L) (where L = N_2, **1**; CN^{t}Bu, **4**; CO, **6**) can facilitate heterolytic cleavage of H_2 and of the C(sp)-H and C(sp^2)-H bonds of arylacetylenes and formaldehyde, respectively, resulting in Fe-B bond rupture and formal hydride transfer to the boron of the ligand scaffold. The formal hydride transfer from the C(sp)-H of arylacetylenes to give iron-acetylide complexes is distinct from traditional syntheses of metal-acetylide complexes in that a hydride equivalent is formally abstracted by the Lewis acidic borane unit in **1** from a C(sp)-H hydrogen.[25]

Dihydrogen addition across the Fe-B bond is reversible, and the boron is also capable of shuttling the hydride equivalent derived from H_2 to unsaturated substrates under stoichiometric hydrogenation conditions. The hydrogen chemistry of this (TPB)Fe(L) system contrasts with the related nickel[26] and cobalt[24] complexes of TPB, where the metal-boron bond remains intact under an H_2 atmosphere.

An understanding of the factors that govern metal-boron bond cleavage will aid in the development of cooperative catalytic reactions in metallaboratranes. The direct role, if any, of the borane ligand in assisting the H_2 cleavage step is an interesting question in this context for the present iron and recently reported diphosphine-borane-iron systems,[27] and also conceptually related to the nickel system (Scheme 1).[10] Determining whether there is a cooperative interaction between the coordinated H_2 ligand, the iron center, and the borane subunit en route to H-H cleavage (and its microscopic reverse), akin to H-H cleavage by frustrated Lewis pairs,[9] calls for detailed theoretical studies that are the subject of ongoing research.

EXPERIMENTAL

General Considerations

All manipulations were carried out using standard glovebox or Schlenk techniques under an N_2 atmosphere. Unless otherwise noted, solvents were deoxygenated and dried by thoroughly sparging with N_2 gas followed by passage through an activated alumina column in the solvent purification system by SG Water, USA LLC. Deuterated solvents and D_2 gas were purchased from Cambridge Isotope Laboratories, INC. The deuterated solvents were degassed and dried over activated 3 Å sieves prior to use. Unless otherwise noted, all compounds were purchased commercially and used without further purification. TPB,[13] (SiP^{i}Pr$_3$)Fe(Me),[19] (SiP^{i}Pr$_3$)Fe(N_2)(H),[17] and monodeuterated phenyl- and tolylacetylene (PhC_2D and TolC_2D)[28] were synthesized by literature procedures. Elemental analyses were performed by Midwest Microlab, LLC., Indianapolis, IN.

NMR spectra were recorded on Varian 300 MHz, 400 MHz, and 500MHz spectrometers. ^{1}H and ^{13}C chemical shifts are reported in ppm relative to residual solvent as internal standards. ^{31}P and ^{11}B chemical shifts are reported in ppm relative to 85% aqueous H_3PO_4 and $BF_3{\cdot}Et_2O$, respectively. Multiplicities are indicated by br (broad), s (singlet), d (doublet), t (triplet), quart (quart), quin (quintet), multiplet (m), d-d (doublet-of-doublets), and t-d (triplet-of-doublets).

FT-IR measurements were obtained on samples prepared as KBr pellets or in solution using a Bio-Rad Excalibur FTS 300 spectrometer with Varian Resolutions Pro software at 4 cm^{-1}

NIH-PA Author Manuscript

NIH-PA Author Manuscript

NIH-PA Author Manuscript

resolution. The ATR-IR measurements were measured on a thin film of the complex obtained from evaporating a drop of the solution on the surface of a Bruker APLHA ATR-IR Spectrometer probe (Platinum Sampling Module, diamond, OPUS software package) at 2 cm^{-1} resolution. IR intensities indicated by s (strong), m (medium), and w (weak).

X-ray Crystallography

X-ray diffraction was measured on the Bruker Kappa Apex II diffractometer with Mo Kα radiation. Structures were solved using the SHELXS software and refined against F^2 on all data sets by full matrix least squares with SHELXL. The crystals were mounted on a glass fiber with Paratone oil.

Computational Methods

Geometry optimizations were performed using the Gaussian03 package. B3LYP exchange-correlation functional was employed with a 6-31G(d) basis set. The GDIIS algorithm was used. A full frequency calculation was performed on each structure to ensure that they were the true minima. A single negative vibrational frequency was observed for the transition state between **3** and its equatorial-H_2 isomer, confirming that this structure was the transition state. See SI for full a description of the computational method.

HD Gas Generation

D_2O (1mL) was added to an evacuated, cooled sample (−78 °C) of solid lithium aluminum hydride (316 mg, 8.2 mmol) in a Schlenk flask. An evacuated Schlenk line was filled with the resulting HD gas (*ca.* 1 atm) as the Schlenk flask was warmed to room temperature. A J-Young NMR tube containing a freeze-pump-thawed solution was the respective complex was exposed to the HD gas.

Synthesis of (TPB)(μ-H)Fe(N_2)(H) (2)—A J-Young NMR tube containing a brown-red solution **1** (20.3 mg, 31.1 mmol) in C_6H_6 (0.8 mL) was freeze-pump-thawed (3x) and, with the J-Young tube frozen with liquid nitrogen, exposed to H_2 (1.2 equiv). The solution was thawed and mixed, giving a yellow solution. An atmosphere of N_2 was subsequently introduced and the reaction was mixed for 2 h to yield **2** (100% yield by ^{1}H NMR spectroscopy with a ferrocene integration standard). Alternatively, **2** could be synthesized from **3** by degassing a solution of **3** of free H_2 by freeze-pump-thaw (3x), exposing it to an N_2 atmosphere, and mixing the solution overnight (100% yield by ^{1}H NMR spectroscopy with a ferrocene integration standard). Yields could not be determined by mass because **2** was unstable to prolonged exposure to dynamic vacuum. Yellow-orange XRD quality crystals were grown in a concentrated solution of pentane:THF (10:1) at −30 °C. ^{1}H NMR (C_6D_6, 300 MHz): δ 7.9 (2H, d, $^3J_{H\text{-}H}$ = 6 Hz, Ar-*H*), δ 7.7 (1H, br s, Ar-*H*), δ 7.3 (3H, d, $^3J_{H\text{-}H}$ = 6 Hz, Ar-*H*), δ 7.0 (3H, t, $^3J_{H\text{-}H}$ = 9 Hz, Ar-*H*), δ 2.7 (4H, d, $^2J_{P\text{-}H}$ = 18 Hz, PC*H*), δ 2.4 (2H, br s, PC*H*), δ 1.4 (6H, d,$^3J_{H\text{-}H}$ = 6 Hz, CH_3), δ 1.3 (12H, br s, CH_3), δ 1.1 (6H, d-d, $^3J_{P\text{-}H}$ = 15 Hz, $^3J_{H\text{-}H}$ = 6 Hz, CH_3), δ 0.8 (6H, d, $^3J_{P\text{-}H}$ = 9 Hz, CH_3), δ − 9.6 (1H, d-t, $^2J_{H\text{-}P\,cis}$ = 81 Hz, $^2J_{H\text{-}P\,trans}$ = 36 Hz, Fe-*H*), δ −30.4 (1H, s, Fe-(μ-*H*)-B). ^{2}H NMR (C_6H_6/C_6D_6, 76 MHz): δ −9.5 (1D, br s), δ −30.3 (1D, br s). ^{31}P NMR (C_6D_6, 121 MHz): δ 73.6 (2P, s), δ 64.2 (1P, s). ^{13}C NMR (C_6D_6, 125 MHz): δ 161.9 (s, C^{Ar}), δ 143.5 (s, C^{Ar}), δ 141.0 (s, C^{Ar}), δ 132.3 (s, C^{Ar}), δ 131.8 (s, C^{Ar}), δ 131.3 (s, C^{Ar}), δ 130.3 (s, C^{Ar}), δ 124.6 (s, C^{Ar}), δ 124.0 (s, C^{Ar}), δ 32.0 (s, P*C*H), δ 29.4 (s, P*C*H), δ 28.5 (s, P*C*H), δ 22.8 (s, *C*H_3), δ 20.1 (s, *C*H_3), δ 19.7 (s, *C*H_3), δ 18.9 (s, *C*H_3). ^{11}B NMR (C_6D_6, 128 MHz): δ 8.2 (br). IR (KBr, cm^{-1}): 2071 (s, N≡N), 1960 (w) 1934 (w). UV-vis (THF, nm {M^{-1} cm^{-1}}): 328 {shoulder, 500}, 280 {shoulder, 11250}. Anal.: Elemental analysis could not be obtained because of the instability of the compound under dynamic vacuum.

NIH-PA Author Manuscript

NIH-PA Author Manuscript

NIH-PA Author Manuscript

Synthesis of (TPB)(μ-H)Fe(H_2)(H) (3)—A J-Young NMR tube containing a brown-red solution **1** (21 mg, 31.1 mmol) in C_6H_6 (0.8 mL) was freeze-pump-thawed (3x). Upon warming to room temperature, the sample was exposed to H_2 (1 atm), resulting in a clear yellow solution. The reaction was mixed for 24 h to give **3** (100% by ^{1}H NMR spectroscopy with a ferrocene integration standard). The yield could not be determined by weight because **3** was unstable to prolonged exposure to dynamic vacuum. Yellow-orange XRD quality crystals were grown under 1 atm of H_2 in a concentrated solution of pentane:THF (10:1) at −78 °C. ^{1}H NMR (C_6D_6, 300 MHz): δ 8.0 (3H, d, $^3J_{H-H}$ = 6 Hz, Ar-*H*), δ 7.3 (3H, t, $^3J_{H-H}$ = 9 Hz, Ar-*H*), δ 7.2 (3H, t, $^3J_{H-H}$ = 9 Hz, Ar-*H*), δ 7.0 (3H, d, $^3J_{H-H}$ = 6 Hz, Ar-*H*), δ 4.47 (s, free H_2), δ 2.3 (6H, m, PC*H*), δ 1.0 (18H, d-d, $^3J_{H-P}$ = 15 Hz, $^3J_{H-H}$ = 6 Hz, CH_3), δ 0.8 (18H, d-d, $^3J_{H-P}$ = 15 Hz, $^3J_{H-H}$ = 6 Hz, CH_3), δ −15.1 (br s, 2H). T_{1min} (d_8-toluene): 35 ms (δ −15.1, −32 °C). ^{2}H NMR (C_6H_6/C_6D_6, 76 MHz): δ −15.4 (1D, br s). ^{31}P NMR (C_6D_6, 121 MHz): δ 90.0 (3P, s). ^{13}C NMR (C_6D_6, 125 MHz): δ 163.5 (s, C^{Ar}), δ 144.6 (s, C^{Ar}), δ 144.1 (s, C^{Ar}), δ 130.9 (d, J_{P-C} = 23 Hz, C^{Ar}), δ 124.5 (s, C^{Ar}), δ 123.9 (s, C^{Ar}), δ 28.6 (s, P*C*H), δ 21.2 (s, *C*H_3), δ 19.9 (s, *C*H_3). ^{11}B NMR (C_6D_6, 128 MHz): δ 7.5 (br). IR (KBr, cm^{-1}): 2278 (w), 19618 (w), 1845 (w). UV-vis (THF, nm {M^{-1} cm^{-1}}): 377 {shoulder, 1532}, 275 {14532}. Anal.: Elemental analysis could not be obtained because of the instability of the compound under dynamic vacuum.

Synthesis of (TPB)Fe(CN^{t}Bu) (4)—*Tert*-butyl isocyanide (20 mg, 0.24 mmol) was added to a brown solution of (TPB)Fe(N_2) (40 mg, 59 μmol) in benzene (2 mL), causing an instantaneous darkening upon gentle shaking. The volatiles were removed by lyophilization and the residue was extracted with tetramethylsilane (2 mL). The resulting dark brown solution was slowly concentrated down to *ca.* 0.2 mL by vapor diffusion into hexamethyldisiloxane. Removal of the mother liquor by decantation, washing with cold tetramethylsilane (2 × 0.1 mL) and drying *in vacuo* afforded (TPB)Fe(CN^{t}Bu) as brown crystals (33 mg, 77%). ^{1}H NMR (C_6D_6, 300 MHz): δ 11.2 (3H), δ 9.2 (3H), δ 8.6 (3H), δ 8.5 (9H), δ 6.4 (3H), δ 5.2 (9H), δ 3.7 (12H), δ 2.9 (9H), δ −1.5 (9H), δ −2.3 (3H). IR (KBr, cm^{-1}): 1972 (C≡N). UV-Vis (THF, nm {$cm^{-1}M^{-1}$}): 600 {shoulder, 428}, 910 {70}. μ_{eff} (C_6D_6, method of Evans, 20 °C): 1.7 μ_B. Anal.: Calc'd for $C_{41}H_{64}BFeNP_3$: C 67.50, H 8.70, N 1.92; found: C 67.20, H 8.54, N 1.72.

Synthesis of (TPB)(μ-H)Fe(CN^{t}Bu)(H) (5)—A heavy-walled Schlenk tube containing a yellow-brown solution of **4** (16.4 mg, 22.4 mmol) in C_6H_6 (10 mL) was freeze-pump-thawed (3x). Upon warming to room temperature, the sample was exposed to H_2 (1 atm) for a few minutes. The Schlenk tube was sealed and heated under vigorous mixing at 40 °C for 85 h. Removal of the solvent *in vacuo*, extraction with C_6H_6, and lyophilization yielded a solid of **5** (17.3 mg, 98 %). Room temperature evaporation of a solution of **5** in a diethyl ether:pentane (2 mL to 1 mL) mixture yielded yellow crystals suitable for XRD analysis. ^{1}H NMR (C_6D_6, 300 MHz): δ 8.1 (1H, d, $^3J_{H-H}$ = 9 Hz, Ar-*H*), δ 7.4 (3H, d, $^3J_{H-H}$ = 9 Hz, Ar-*H*), δ 7.2 (3H, d, $^3J_{H-H}$ = 6 Hz, Ar-*H*), δ 7.1 (3H, d, $^3J_{H-H}$ = 9 Hz, Ar-*H*), δ 2.7 (2H, br s, PC*H*), δ 2.5 (2H, br s, PC*H*), δ 2.2 (2H, t, $^2J_{H-P}$ = 9 Hz, PC*H*), δ 1.3 (16H, m, CH_3), δ 1.1 (9H, s, C(CH_3)$_3$), δ 1.0 (6H, d, $^3J_{H-H}$ = 6 Hz, CH_3), δ 0.8 (6H, d-d, $^3J_{H-P}$ = 15 Hz, $^3J_{H-H}$ = 6 Hz, CH_3), δ 0.7 (6H, br s, CH_3), δ −11.7 (1H, t-d, $^2J_{H-P\,cis}$ = 87 Hz, $^2J_{H-P\,trans}$ = 27 Hz, Fe-*H*), δ −23.9 (1H, br s, Fe-(μ-*H*)-B). ^{13}C NMR (C_6D_6, 125 MHz): δ 176.9 (quart, $^2J_{C-P}$ = 8 Hz, *C*N^{t}Bu), δ 163.5 (br s, C^{Ar}), δ 163.0 (br s, C^{Ar}), δ 144.9 (m, C^{Ar}), δ 143.0 (d, J_{C-P} = 20 Hz, C^{Ar}), δ 131.9 (d, $^2J_{C-P}$ = 7.5 Hz, C^{Ar}), δ 130.6 (d, J_{C-P} = 3.2 H, C^{Ar}), δ 130.5 (d, J_{C-P} = 2.5 H, C^{Ar}), δ 128.6 (s, C^{Ar}), δ 127.5 (s, C^{Ar}), δ 124.2 (s, C^{Ar}), δ 123.6 (s, C^{Ar}), δ 55.3 (s, *C*(CH_3)$_3$), δ 31.6 (s, P*C*H), δ 30.9 (s, P*C*H), δ 29.2 (m, P*C*H), δ 28.5 (d, $^2J_{C-P}$ = 7.5 Hz, P*C*H), δ 23.8 (s, *C*H_3), δ 20.4 (s, *C*H_3), δ 20.3 (m, *C*H_3), δ 20.2 (s, *C*H_3), δ 19.9 (s, *C*H_3), δ 19.7 (s, *C*H_3). ^{31}P NMR (C_6D_6, 121 MHz): δ 81.3 (2P, d, $^2J_{P-P}$ = 63 Hz), δ 72.4 (1P, s). IR (KBr, cm^{-1}): 2027 (s, C≡N), 1942 (w, Fe-H). UV-Vis (THF, nm {cm^{-1} M^{-1}}): 205 {5530},

NIH-PA Author Manuscript NIH-PA Author Manuscript NIH-PA Author Manuscript

224 {15437}, 245 {17142}, 255 {16635}, 285 {4117}, 335 {shoulder, 2166}, 400 {1830}. Anal: Calc'd for $C_{41}H_{66}BFeNP_3$: C 67.32, H 8.96, N 1.91; found: C 66.59, H 8.61, N 1.30.

Synthesis of (TPB)(μ-H)Fe(CO)(H) (7) from 6 and H_2—In a J-Young NMR tube, **6** (6.0 mg, 8.9 μmol) was dissolved in C_6H_6 (0.7 mL) to give a brown-red solution. The solution was freeze-pump-thawed (3x) and subsequently exposed to H_2 (1 atm) for *ca.* 5 min. The reaction was then heated at 80 °C for 5 days, during which time a clear yellow solution developed. Removal of the solvent *in vacuo*, extraction with C_6H_6, and lyophilization yielded a yellow solid of **7** (5.9 mg, 98 %). Room temperature evaporation of a solution of **7** in a diethyl ether:pentane (1 mL to 0.5 mL) mixture yielded yellow analytically pure **7**. ^{1}H NMR (C_6D_6, 300 MHz): δ 8.1 (2H, d, $^3J_{H-H}$ = 6 Hz, Ar-*H*), δ 7.9 (1H, d, $^2J_{P-H}$ = 9 Hz, Ar-*H*), δ 7.2 (4H, m, Ar-*H*), δ 7.0 (4H, m, Ar-*H*), δ 2.6 (2H, t, $^2J_{H-P}$ = 3 Hz, PC*H*), δ 2.4 (2H, q, $^2J_{H-P}$ = 6 Hz, PC*H*), δ 2.2 (2H, t, $^2J_{H-P}$ = 6 Hz, PC*H*), δ 1.4 (6H, d, $^3J_{H-P}$ = 6 Hz, CH_3), δ 1.2 (12H, m, CH_3), δ 0.9 (6H, d, $^3J_{H-P}$ = 6 Hz, CH_3), δ 0.8 (6H, d-d, $^3J_{H-P}$ = 8 Hz, $^3J_{H-H}$ = 6 Hz, CH_3), δ 0.6 (6H, d, $^3J_{H-P}$ = 6 Hz, CH_3). δ −11.6 (1H, t-d, $^2J_{H-P\,cis}$ = 81 Hz, $^2J_{H-P\,trans}$= 21 Hz, Fe-*H*), δ −20.0 (1H, br s, Fe-(μ-*H*)-B). ^{2}H NMR (C_6H_6, 76 Hz): δ −12.3 (1D, t, $^2J_{P-D}$ = 10 Hz), δ −20.8 (1D, br s). ^{13}C NMR (THF with 1 drop of C_6D_6, 125 MHz): δ 222.7 (br s, *C*O), δ 161.8 (br s, C^{Ar}), δ 142.9 (br s, $^1J_{C-P}$ = 19 Hz, C^{Ar}), δ 140.8 (br s, $^2J_{C-P}$ = 16 Hz, C^{Ar}), δ 131.0 (s, C^{Ar}), δ 129.8 (s, C^{Ar}), δ 128.5 (s, C^{Ar}), δ 128.0 (s, C^{Ar}), δ 124.0 (s, C^{Ar}), δ 123.4 (s, C^{Ar}), δ 30.8 (s, P*C*H), δ 28.3 (s, P*C*H), δ 27.7 (s, P*C*H), δ 22.3 (s, *C*H_3), δ 19.1 (s, *C*H_3), δ 18.8 (s, *C*H_3), δ 18.1 (s, *C*H_3). ^{31}P NMR (C_6D_6, 121 MHz): δ 83.4 (2P, d, $^2J_{P-H}$ = 21 Hz), δ 72.8 (1P, s). IR (KBr, cm^{-1}): 1898 (s, C≡O), 1967 (w, Fe-H). UV-Vis (THF, nm {cm^{-1}M^{-1}}): 270 {4333}, 280 {4111}, 390 {1400}. Anal.: Calc'd for $C_{37}H_{56}BFeOP_3$: C 65.70, H 8.34; found: C 65.64, H 8.08.

Synthesis of (TPB)(μ-H)Fe(CO)(H) (7) from Formaldehyde—Compound **1** (8 mg, 11.8 μmol) or **2** (6 mg, 8.9 μmol) was mixed with excess paraformaldehyde in C_6H_6 for 3 h to give a turbid, light yellow solution. The excess paraformaldehyde was filtered away and the solution was pumped down to give **7** as a yellow solid (from **1**, 8 mg, 100%; from **2**, 7 mg, 100%). Spectroscopic data is identical to those listed above.

Synthesis of (TPB)Fe(C_2H_4) (8)—A J-Young NMR tube containing an orange solution of **3** (8.4 mg, 12.5 μmol) in C_6H_6 (0.8 mL) was freeze-pump-thawed (3x) and exposed to ethylene gas (1 atm) for *ca.* 1 minute. Mixing immediately gave a brown solution of **8**. Removal of solvent *in vacuo* yielded a brown solid (8.3 mg, 99%) of **8**. Dissolution of this solid under N_2 atmosphere gave mostly **8** and small amounts of **1**. Over time, **8** in solution converted to **1**. Crystals suitable for XRD were grown in a saturated, cold pentane:diethyl ether (2:1) solution under an ethylene atmosphere. ^{1}H NMR (C_6D_6, 300 MHz): δ 33.1 (1H), δ 28.8 (1H), δ 18.7 (4H), δ 13.3 (1H), δ 5.25 (s, free C_2H_4), δ 4.9 (3H), δ 4.1 (1H), δ 1.9 (2H), δ −3.0 (10H), δ −6.2 (11H), δ −9.2 (11H), δ −10.0 (3H). UV-Vis (THF, nm {cm^{-1}M^{-1}}): 309 {shoulder, 6032}, 553 {1804}, 938 {418}. μ_{eff} (C_6D_6, method of Evans, 20 °C): 3.2 μ_B (S = 1). Anal.: Elemental analysis could not be obtained because of the instability of the compound under dynamic vacuum.

Synthesis of (TPBH)Fe(C_2Ph) (9)—Phenylacetylene (40.8 mg, 400 μmol) was added to a C_6H_6 solution (5 mL) of **3** (9.0 mg, 13 μmol), immediately giving a gray solution. Removal of the solvent *in vacuo* yielded a black powder of **9** (10 mg, 100%). ^{1}H NMR (C_6D_6, 300 MHz): δ 28.8 (3H), δ 13.1 (4H), δ 4.7 (18H), δ 2.6 (2H), δ 2.3 (4H), δ 1.2 (2H), δ −29.3 (1H), δ −30.9 (5H). μ_{eff} (C_6D_6, method of Evans, 20 °C): 5.1 μ_B (S = 2). UV-Vis (THF, nm {cm^{-1}M^{-1}}): 325 {20670}, 439 {1051}, 479 {971}, 522 {955}, 601 (br abs extending from 400 to 700 nm, 930}, 883 {1466}. IR (KBr, cm^{-1}): 2040 (s, C≡C), 2490 (m, B-H). Anal.: Calc'd for $C_{44}H_{60}FeP_3B$: C, 70.60; H, 8.08. Found: C, 70.39; H, 7.89.

NIH-PA Author Manuscript

NIH-PA Author Manuscript

NIH-PA Author Manuscript

Synthesis of (TPBD)Fe(C_2Ph)—The B-D labeled complex of **9** was generated by the same method described for **9**, except that PhC_2H was replaced with PhC_2D. The ^{1}H NMR spectrum was identical to **10**. IR (thin film, cm^{-1}): 1826 (br m, B-D; predicted 1832).

Synthesis of (TPBH)Fe(C_2Tol) (10)—Tolylacetylene (16.1 mg, 138 μmol) was added to a C_6H_6 solution (5 mL) of **3** (22.9 mg, 33.0 μmol), immediately giving a gray solution. Removal of the solvent *in vacuo* yielded a black powder of **10** (24.0 mg 100%). Black XRD quality crystals of **10** were grown by diffusion of hexamethyldisiloxane into a concentrated THF solution of **10**. ^{1}H NMR (C_6D_6, 300 MHz): δ 44.1 (1H), δ 29.4 (1H), δ 13.3 (1H), δ 4.6 (2H), δ 3.3 (1H), δ 2.7 (2H), δ 2.3 (4H), δ 1.8 (2H), δ −32.3 (1H). μ_{eff} (C_6D_6, method of Evans, 20 °C): 5.2 μ_B (S = 2). UV-Vis (THF, nm {cm^{-1}M^{-1}}): 326 {24476}, 444 {1243}, 486 {1138}, 527 {shoulder, 975}, 624 (915}, 887 {1575}. IR (KBr, cm^{-1}): 2039 (s, C≡C), 2500 (m, B-H). Anal.: Calc'd for $C_{45}H_{62}FeP_3B$: C, 70.88; H, 8.20. Found: C, 70.44; H, 7.80.

Synthesis of (TPBD)Fe(C_2Tol)—The B-D labeled complex of **10** was generated by the same method described for **10**, except that TolC_2H was replaced with TolC_2D. The ^{1}H NMR spectrum was identical to **10**. IR (thin film, cm^{-1}): 1824 (br m, B-D; predicted 1841).

Synthesis of 11—A yellow, C_6H_6 solution of **1** (18.2 mg, 27 μmol) was heated in a J-Young NMR tube under H_2 (1 atm) at 80 °C for 2 h, giving a turbid red-purple solution. The solvent was removed *in vacuo*, and the dark crude material was redissolved in hexamethyldisiloxane (3 mL) and filtered through a glass frit to remove a black solid (presumably iron metal). Removal of the solvent *in vacuo* gave a purple solid that is a mixture of **11** (1 equiv) and diisopropyl-phosphino-benzene (^{i}Pr2PPh, 1 equiv). Orange XRD quality crystals of **11** can be grown from slow evaporation of a concentrated hexamethyldisiloxane solution of **11** at room temperature (5.1 mg, 18%). Dissolution of these crystals by heating in benzene or THF results in decomposition. Therefore, spectral data is reported on the mixture of **11** with ^{i}Pr2PPh. Compound **11** appears to be fluxional at RT. ^{1}H NMR (C_6D_6, 300 MHz): δ 8.4 (4H, s, Ar-*H*), δ 7.6 (4H, s, Ar-*H*), δ 7.5 (3H, d, $^2J_{H-P}$ = 6 Hz, Ar-*H*), δ 2.7 (1H, d, $^2J_{H-P}$ = 6 Hz, PC*H*), δ 2.5 (1H, s, PC*H*), δ 1.9 (1H, quart, $^3J_{H-H}$ = 6 Hz, PC*H*), δ 1.3 (6H, d-d, $^3J_{P-H}$ = 4 Hz, $^3J_{H-H}$ = 2 Hz, CH_3), δ 1.2 (6H, d, $^3J_{H-H}$ = 3 Hz, CH_3), δ 1.1 (6H, quart, $^3J_{P-H}$ = 4 Hz, $^3J_{H-H}$ = 2 Hz, CH_3), 0.9 (12H, m, CH_3), −17.0 (0.25H, t, $^2J_{H-P}$ = 36 Hz, B-*H*). ^{13}C NMR (C_6D_6, 125 MHz): δ 157.4 (br s, C^{Ar}), δ 144.2 (br s, C^{Ar}), δ 134.9 (d, $^2J_{C-P}$ = 19 Hz, C^{Ar}), δ 130.5 (s, C^{Ar}), δ 129.3 (s, C^{Ar}), δ 125.7 (d, $^2J_{C-P}$ = 23 Hz, C^{Ar}), δ 25.5 (br s, P*C*H), δ 24.9 (br s, P*C*H), δ 24.4 (br s, P*C*H), δ 23.7 (br s, P*C*H), δ 23.1 (br s, P*C*H), δ 20.0 (m, *C*H$_3$), δ 19.4 (m, *C*H$_3$), δ 18.2 (m, *C*H$_3$). ^{31}P NMR (C_6D_6, 121 MHz): δ 99.1 (4P, s), δ 9.5 (2P, s). ^{11}B NMR (C_6D_6, 128 MHz): δ 41.0 (br). UV-Vis (THF, nm {cm^{-1}M^{-1}}): 264 {shoulder, 31650}, 520 {826}. IR (KBr, cm^{-1}): 2088 (s, B-H), 1838 (m, B-H). Anal.: Calc'd for $C_{51}H_{86}FeP_4B_2Si$ (i.e., **11** + Me_3SiH): C, 65.96; H, 9.33. Found: C, 65.70; H, 9.16.

Synthesis of (SiP$^{iPr}_3$)Fe(H_2)(H)—In a 100 mL Schlenk tube a red solution of (SiP^{i}Pr$_3$)Fe(Me) (1.05 g, 1.547 mmol) in C_6H_6 (50 mL) was degassed by freeze-pump-thaw (3x). H_2 gas (1 atm) was charged into the reaction mixture. The reaction was heated at 60 °C for over a week. The reaction solution was then quickly filtered through Celite and volatiles were removed *in vacuo* to give a light yellow powder. The solid was collected on a glass-frit and washed with pentane (3 mL x 2). The resulting product **(SiP$^{iPr}_3$)Fe(H_2)(H)** (950 mg, 1.425 mmol, 92%) was obtained as a light yellow powder after drying under vacuum. ^{1}H NMR (C_6D_6, 300 MHz): δ 8.3 (3H, d, $^3J_{H-P}$ = 6.8 Hz, Ar-*H*), δ 7.3 (3H, m, Ar-*H*), δ 7.2 (3H, t, $^3J_{H-H}$ = 7.2 Hz, Ar-*H*), δ 7.1 (3H, t, $^3J_{H-H}$ = 7 Hz, Ar-*H*), δ 4.5 (s, free H_2), δ 2.2 (6H, m, PC*H*), δ 1.0 (18H, m, CH_3), δ 0.8 (18H, br s, CH_3), δ 0.16 (s, free CH_4), δ −10.0

NIH-PA Author Manuscript

NIH-PA Author Manuscript

NIH-PA Author Manuscript

(3H, quin, $^2J_{P\text{-}H}$ = 18.4 Hz, Fe-*H*). T_{1min} (d_8-toluene): 32 ms (δ −10.0, −30 °C). ^{31}P NMR (C_6D_6, 121 MHz): δ 100 (br); (d_8-Tol, 300 MHz, −80 °C): δ 117.9 (d, $^3J_{P\text{-}P}$ = 43.5 Hz), δ 94.7 (bs), δ 84.7 (d, $^3J_{P\text{-}P}$ = 43.5 Hz). ^{13}C NMR (THF with 1 drop of C_6D_6, 125 MHz): δ 157.3 (d, $J_{C\text{-}P}$ = 22.5 Hz, C^{Ar}), δ 150.5 (d, $J_{C\text{-}P}$ = 21.3 Hz, C^{Ar}), δ 130.1 (d, $J_{C\text{-}P}$ = 9.3 Hz, C^{Ar}), δ 128.6 (s, C^{Ar}), δ 127.4 (s C^{Ar}), δ 126.0 (d, $J_{C\text{-}P}$ = 2.5 Hz, C^{Ar}), δ 29.0 (br s, P*C*H), δ 20.4 (br s, *C*H$_3$), δ 19.2 (br s, *C*H$_3$), UV-Vis (THF, nm {cm^{-1}M^{-1}}): 353 {3040}. IR (KBr pellet; cm^{-1}): 1941 (w, Fe-H). Anal.: Elemental analysis could not be obtained because of the instability of the compound under prolonged exposure to N_2.

Isotopomers of (SiP$^{iPr}_3$)Fe(H$_2$)(H); (SiP$^{iPr}_3$)Fe(H$_2$)(H), (SiP$^{iPr}_3$)Fe(HD)(H), (SiP$^{iPr}_3$)Fe(H$_2$)(D), (SiP$^{iPr}_3$)Fe(D$_2$)(H), (SiP$^{iPr}_3$)Fe(HD)(D), and (SiP$^{iPr}_3$)Fe(D$_2$)(D): HD gas was generated by the method described above and charged into a J-young tube containing a degassed solution of **SiP$^{iPr}_3$)Fe(Me)** in C_6D_6. The solution was heated at 60 °C for over a week. Monitoring the progress of the reaction by ^{1}H NMR revealed the gradual disappearance of **1** and formation of diamagnetic isotopomers **(SiP$^{iPr}_3$)Fe(H$_2$)(H)**. Spectroscopic features in the ^{1}H NMR spectrum were identical to **(SiP$^{iPr}_3$)Fe(H$_2$)(H)** except for the hydridic proton resonances, where isotopologues were observed. ^{1}H{^{31}P} NMR (C_6D_6, 300 MHz): δ −10.0 (3H, quart, $^2J_{P\text{-}H}$ = 18.4 Hz, H$_3$), δ −10.0 (t, $^1J_{H\text{-}D}$ = 9.5 Hz, H$_2$D), δ −10.23 (quin, $^1J_{H\text{-}D}$ = 9.3 Hz, HD$_2$).

Synthesis of (SiP$^{iPr}_3$)Fe(CO)(H)—In a 50 mL Schlenk tube a yellow solution of **(SiP$^{iPr}_3$)Fe(H$_2$)(H)** (330 mg, 0.495 mmol) in C_6H_6 (20 mL) was freeze-pump-thawed (3x). The solution was charged with CO (1 atm). The reaction was mixed overnight at RT and then for 1 h at 60 °C, resulting in a light yellow solution. After completion, the solution was degassed by freeze-pump-thaw (3x). The solution was filtered through Celite, and the volatiles were removed *in vacuo* to give a light yellow powder. The solid was collected on a glass-frit and washed with pentane (5 mL x 3). Removal of the solvent *in vacuo* yields **(SiP$^{iPr}_3$)Fe(CO)(H)** (266 mg, 0.384 mmol, 78%) as a light yellow powder. Crystals suitable for X-ray diffraction were obtained by RT evaporation of a pentane solution of **(SiP$^{iPr}_3$)Fe(CO)(H)**. ^{1}H NMR (d_8-toluene, 300 MHz): δ 8.2 (2H, d, $^3J_{H\text{-}H}$ = 7.2 Hz), δ 8.1 (1H, d, $^3J_{H\text{-}H}$ = 7.2 Hz), δ 7.3 (3H, m), δ 7. 2 (3H, m), δ 7.1 (3H, m), δ 2.7 (2H, m), δ 2.4 (2H, m), δ 2.2 (2H, m), δ 1.5 (6H, d-d, $^3J_{H\text{-}P}$ = 15.2 Hz, $^3J_{H\text{-}P}$ = 6.8 Hz), δ 1.3 (6H, m), δ 1.1 (6H, d-d, $^3J_{H\text{-}P}$ = 12.6 Hz, $^3J_{H\text{-}H}$ = 6.6 Hz), δ 0.8 (12H, m), δ 0.5 (6H, s), δ −14.9 (1H, t-d, $^3J_{H\text{-}Pcis}$ = 81.0 Hz, $^3J_{H\text{-}Ptrans}$ = 14.1 Hz). ^{31}P NMR (C_6D_6, 121 MHz, RT): δ 88.0 (br), δ 90.0 (s); (d_8-toluene, 121 MHz, −80 °C): δ 109.9 (t, $^3J_{P\text{-}P}$ = 65 Hz, $^3J_{P\text{-}H}$ = 80 Hz), δ 90.0 (s), δ 77.9 (t, $^3J_{P\text{-}P}$ = 65 Hz, $^3J_{P\text{-}H}$ = 80 Hz). ^{13}C NMR (THF with 1 drop of C_6D_6, 125 MHz): δ 223.0 (d, $^2J_{C\text{-}P}$ = 6.3 Hz, *C*O), δ 157.2 (d, $J_{C\text{-}P}$ = 8.8 Hz, C^{Ar}), δ 155.2 (d, $J_{C\text{-}P}$ = 10.6 Hz, C^{Ar}), δ 150.5 (d, $J_{C\text{-}P}$ = 11.3 Hz, C^{Ar}), δ 150.2 (d, $J_{C\text{-}P}$ = 8.8 Hz, C^{Ar}), δ 148.6 (d, $J_{C\text{-}P}$ = 18.1 Hz, C^{Ar}), δ 132.4 (d, $J_{C\text{-}P}$ = 9.4 Hz, C^{Ar}), δ 131.9 (d, $J_{C\text{-}P}$ = 8.8 Hz, C^{Ar}), δ 130.9 (s, C^{Ar}), δ 128.3 (s, C^{Ar}), δ 128.5 (s, C^{Ar}), δ 127.1 (s, C^{Ar}), δ 126.8 (s, C^{Ar}), δ 126.4 (s, C^{Ar}), δ 125.8 (s, C^{Ar}), δ 124.7 (s, C^{Ar}), δ 32.4 (s, P*C*H), δ 30.7 (s, P*C*H), δ 30.0 (s, P*C*H), δ 29.6 (s, P*C*H), δ 28.7 (s, P*C*H), δ 22.8 (s, *C*H$_3$), δ 22.1 (s, *C*H$_3$), δ 20.2 (s, *C*H$_3$), δ 19.5 (s, *C*H$_3$), δ 19.2 (s, *C*H$_3$), δ 19.1 (s, *C*H$_3$), δ 18.9 (s, *C*H$_3$), δ 18.0 (s, *C*H$_3$). UV-Vis (THF, nm {cm^{-1}M^{-1}}): 340 {2,050}, 400 {1,500}. IR (KBr pellet; cm^{-1}): 1882 (s, C≡O), 1944 (m, Fe-H). Anal.: Calc'd for $C_{37}H_{57}FeOP_3Si$: C, 64.16; H, 8.00. Found: C, 64.15; H, 8.13.

Synthesis of (SiP$^{iPr}_3$)Fe(^{13}CO)(H)—In a J-Young NMR tube an orange C_6D_6 solution of **(SiP$^{iPr}_3$)Fe(H$_2$)(H)** was degassed by three freeze-pump-thaw (3x). Subsequently, ^{13}CO (1 atm) was added and the reaction was allowed to mix overnight at RT. The ^{1}H NMR spectrum was identical to **(SiP$^{iPr}_3$)Fe(CO)(H)**. IR (KBr; cm^1): 1836 (s, ^{13}C≡O).

NIH-PA Author Manuscript

NIH-PA Author Manuscript

NIH-PA Author Manuscript

Generation of (TPBH)Fe(Et) (A)

Compound **A** was observed as an intermediate of catalytic ethylene hydrogenation under the reaction conditions described in section "Catalytic Hydrogenation Studies." We were also able to generate **A** starting from complex **8.** This procedure described below is more amendable to observing **A** spectroscopically. A dark yellow C_6D_6 solution (0.5 mL) of **8** (2.8 mg, 4.2 μmol) under ethylene (1 atm) in a J-Young tube was frozen (−196 °C) and H_2 was added (1 atm). The reaction was thawed and quickly mixed only *immediately* prior to measuring the ^{1}H NMR spectrum, revealing a mixture of **8** and **A**. Further mixing of the solution for *ca.* 45 min yielded a purple solution of **A** with a small residual amount of **8** by ^{1}H NMR spectroscopy. Free C_2H_4, C_2H_6, and H_2 were also observed in the ^{1}H NMR spectrum. Compound **A** could not be isolated as a solid due its instability. For example, an ATR IR spectrum of a thin film of the reaction mixture obtained by solvent evaporation under an N_2 atmosphere over a period less than 30 sec gave vibrational bands diagnostic of **1**, **2**, and **A**. ^{1}H NMR (C_6D_6, 300 MHz): δ 17.3 (1H), δ 6.6 (1H), δ 5.26 (s, free C_2H_4), δ 4.4 (1H), δ 4.47 (br s, free H_2), δ 3.3 (2H), 0.80 (s, free C_2H_6), δ −1.9 (8H), δ −5.5 (6H). IR (thin film; cm^{-1}): 2470 (br s, B-H of **A**), 2069 (m, N≡N of (TPB)(μ-H)Fe(N_2)(H) **2**), 2009 (s, N≡N of (TPB)Fe(N_2) **1**). UV-Vis, obtained 45 min after exposing **A** under 1 atm of ethylene to 1 atm of H_2 (THF, nm {$cm^{-1}M^{-1}$}): 325 {20670}, 439 {1051}, 479 {971}, 522 {955}, 601 (br abs extending from 400 to 600 nm, 930}, 883 {1466}. Magnetic data could not be obtained due to residual **10** in the reaction mixture. Anal.: Elemental analysis could not be obtained because of the instability of the compound under dynamic vacuum.

Catalytic Hydrogenation Studies

Compound **1** (0.045 g, 0.07 mmol) and ferrocene (0.012 g, 0.07 mmol) were dissolved in 1.5 mL of C_6D_6, giving a 0.045 M precatalyst stock solution. Ferrocene was used as an internal ^{1}H NMR integration standard and did not affect the rates of hydrogenation. For a catalytic run, 0.1 mL of the stock solution was taken and mixed with 0.35 mL of C_6D_6, and 30 equiv of substrate in a J-Young NMR tube (3.2 mL capacity). For styrene hydrogenation, this equates to 0.01 M **1** and 0.3 M styrene. For phenylacetylene hydrogenation, this equates to 0.01 M **1** and 0.29 M phenylacetylene. For ethylene hydrogenation, this equates to 0.01 M **1** and 0.30 M ethylene. The sample in the J-Young NMR tube was subsequently degassed by freeze-pump-thaw (3x) and backfilled with 1 atm H_2 (0.11 mmol). The J-Young NMR tube was continually inverted (12 min^{-1}) to ensure adequate mass transfer. The tube was periodically refilled with H_2 to maintain 1 atm of H_2. All reactions were monitored periodically by ^{1}H NMR spectroscopy until >95% completion. All reactions resulted in clean conversion of the substrate to the corresponding product. Catalytic runs in the presence of a drop of mercury or in the absence of ambient laboratory light had no affect on the reactions. Catalytic hydrogenations could also be cleanly effected by pre-generating **2** or **3** before the addition of the substrate.

Supplementary Material

Refer to Web version on PubMed Central for supplementary material.

Acknowledgments

We acknowledge the Gordon and Betty Moore Foundation and the NIH (GM070757) for funding. M.-E.M acknowledges a Fellowship for Advanced Researchers from the Swiss National Science Foundation. Dr. Charlene Tsay and Lawrence Henling are acknowledged for assistance with X-ray crystallography, and Dr. David VanderVelde is acknowledged for assistance with NMR spectroscopy. We acknowledge the Gordon and Betty Moore Foundation, the Beckman Institute, and the Sanofi-Aventis BRP at Caltech for their generous support of the Molecular Observatory.

NIH-PA Author Manuscript NIH-PA Author Manuscript NIH-PA Author Manuscript

References

1. Hartwig, JF. Organotransition Metal Chemistry: From Bonding to Catalysis. University Science Books; 2010.
2. Bullock, RM., editor. Catalysis Without Precious Metals. Wiley-VCH; 2010.
3. For representative examples of mid-to-late first row transition metal catalysts that perform two-electron transformations see: Bolm C, Legros J, Le Paih J, Zani L. Chem Rev. 2004; 104:6217–6254. [PubMed: 15584700] Hu X. Chem Sci. 2011; 2:1867–1886.Knijnenburg Q, Horton AD, van der Heijden H, Kooistra TM, Hetterscheid DGH, Smits JMM, de Briun B, Budzelaar PHM, Gal AW. J Mol Catal A. 2005; 232:151–159.Tondreau AM, Atienza CCH, Weller KJ, Nye SA, Lewis KM, Delis JGP, Chirik PJ. Science. 2012; 335:567–570. [PubMed: 22301315] Daida EJ, Peters JC. Inorg Chem. 2004; 43:7474–7585. [PubMed: 15530098] Federsel C, Boddien A, Jackstell R, Jennerjahn R, Dyson PJ, Scopelliti R, Laurenczy G, Beller M. Angew Chem, Int Ed. 2010; 49:9777–9780.
4. (a) Noyori R, Yamakawa M, Hashiguchi S. J Org Chem. 2001; 66:7931–7944. [PubMed: 11722188] (b) Morris RH. Chem Soc Rev. 2009; 38:2282–2291. [PubMed: 19623350] (c) Chakraborty S, Guan H. Dalton Trans. 2010; 39:7427–7436. [PubMed: 20505877] (d) Casey CP, Guan H. J Am Chem Soc. 2007; 129:5816–5817. [PubMed: 17439131] (e) Sui-Seng C, Freutel F, Lough AJ, Morris RH. Angew Chem, Int Ed. 2008; 47:940–943.(f) Langer R, Leitus G, Ben-David Y, Milstein D. Angew Chem, Int Ed. 2011; 50:2120–2124.
5. Tsoureas N, Kuo YY, Haddow MF, Owen GR. Chem Comm. 2011; 47:484–486. [PubMed: 20938529]
6. For discussions on the M-B bonding situation: Sircoglou M, Bontemps S, Mercy M, Saffon N, Takahashi M, Bouhadir G, Maron L, Bourissou D. Angew Chem, Int Ed. 2007; 46:8583–8586.Amgoune A, Bourissou D. Chem Comm. 2011; 47:859–871. [PubMed: 21103473] Hill AF. Organometallics. 2006; 25:4741–4743.Parkin G. Organometallics. 2006; 25:4744–4747.
7. (a) Owen GR. Chem Soc Rev. 2012; 41:3535–3546. [PubMed: 22331233] (b) Tsoureas N, Owen GR, Hamilton A, Orpen AG. Dalton Trans. 2008:6039–6044. [PubMed: 19082061]
8. (a) Crossley IR, Foreman MRSt-J, Hill AF, Owen GR, White AJP, Williams DJ, Willis AC. Organometallics. 2008; 27:381–386.(b) Crossley IR, Foreman MRSt–J, Hill AF, White AJ, Williams D. Chem Comm. 2005:221–223. [PubMed: 15724192] (c) Crossley IR, Hill AF, Willis AC. Organometallics. 2007; 26:3891–3895.(d) Crossley IR, Hill AF. Dalton Trans. 2008:201–203. [PubMed: 18097486] (e) Crossley IR, Hill AF, Willis AC. Organometallics. 2008; 27:312–315.(f) Hill AF, Smith MK, Wagler J. Organometallics. 2008; 27:2137–2140.(g) Crossley IR, Hill AF, Willis AC. Organometallics. 2009; 29:326–336.
9. Stephan DW, Erker G. Angew Chem, Int Ed. 2009; 49:46–76.
10. Harman WH, Peters JC. J Am Chem Soc. 2012; 134:5080–5082. [PubMed: 22380492]
11. Kameo H, Nakazawa H. Organometallics. 2012; 31:7476–7484.
12. (a) Moret ME, Peters JC. Angew Chem, Int Ed. 2011; 50:2063–2067.(b) Moret ME, Peters JC. J Am Chem Soc. 2011; 133:18118–18121. [PubMed: 22008018]
13. Bontemps S, Bouhadir G, Dyer PW, Miqueu K, Bourissou D. Inorg Chem. 2007; 46:5149–5151. [PubMed: 17523635]
14. The H-D coupling constant ($J_{H\text{-}D}$) is also in principle an excellent distinguishing characteristic between the η^2-dihydrogen and dihydride ligands.[15] Unfortunately, H-D coupling cannot be resolved in **3**, likely due to fast exchange within the $H_nD_{3\text{-}n}$ unit and H/D scrambling into the methine and terminal methyl positons on the isopropyl groups of the TPB ligand.
15. (a) Desrosiers PJ, Cai L, Lin Z, Richards R, Halpern J. J Am Chem Soc. 1991; 113:4173–4184.(b) Kubas GJ. Chem Rev. 2007; 107:4152–4205. [PubMed: 17927158] (c) Morris RH. Coord Chem Rev. 2008; 252:2381–2394.
16. Van der Sluys LS, Eckert J, Eisenstein O, Hall JH, Huffman JC, Jackson SA, Koetzle TF, Kubas GJ, Vergamini PJ, Caulton KG. J Am Chem Soc. 1990; 112:4831–4841.
17. Lee Y, Kinney RA, Hoffman BM, Peters JC. J Am Chem Soc. 2011; 133:16366–16369. [PubMed: 21954981]
18. Lee Y, Peters JC. J Am Chem Soc. 2011; 133:4438–4446. [PubMed: 21375250]

NIH-PA Author Manuscript

NIH-PA Author Manuscript

NIH-PA Author Manuscript

19. Lee Y, Mankad NP, Peters JC. Nat Chem. 2010; 2:558–565. [PubMed: 20571574]
20. Bartell LS, Roth EA, Hollowell CD, Kuchitsu K, Young JE. J Chem Phys. 1965; 42:2683–2683.
21. Select iron-ethylene complexes of ferracyclopropane character: Zenneck U, Frank W. Angew Chem, Int Ed. 1986; 25:831–833.Schneider JJ, Czap N, Blaser D, Boese R. J Am Chem Soc. 1999; 121:1409–1410.Bennett MA, Ditzel EJ, Hunter AD, Khan K, Kopp MR, Neumann H, Robertson GB, Zeh H. J Chem Soc, Dalton Trans. 2000:1733–1741.Fürstner A, Martin R, Krause H, Seidel G, Goddard R, Lehmann CW. J Am Chem Soc. 2008; 130:8773–8787. [PubMed: 18597432]
22. A similar paramagnetic (S = 2) iron ethyl-hydro-tris(pyrazolyl)borate complex: Shirasawa N, Nguyet TT, Hikichi S, Moro-oka Y, Akita M. Organometallics. 2001; 20:3582–3598.
23. Marchand AP, Marchand NW. Tetrahedron Lett. 1971; 12:1365–1368.
24. Suess DLM, Tsay C, Peters JC. J Am Chem Soc. 2012; 134:14158–14164. [PubMed: 22891606]
25. (a) Reinhard N. Coord Chem Rev. 1982; 47:89–124.(b) Bianchini C, Laschi F, Masi D, Ottaviani FM, Pastor A, Peruzzini M, Zanello P, Zanobini F. J Am Chem Soc. 1993; 115:2723–2730.(c) Field LD, George AV, Malouf EY, Slip IHM, Hambley TW. Organometallics. 1991; 10:3842–3848.
26. Tsay C, Peters JC. Chem Sci. 2012; 3:1313–1318.
27. Suess DLM, Peters JC. J Am Chem Soc. 2013 [Online early access]. 10.1021/ja400836u
28. Rubina M, Gevorgyan V. J Am Chem Soc. 2001; 123:11107–11108. [PubMed: 11686734]

NIH-PA Author Manuscript

NIH-PA Author Manuscript

NIH-PA Author Manuscript

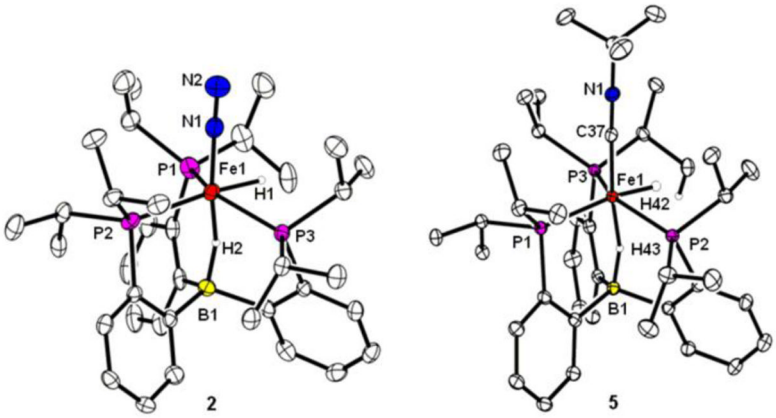

Figure 1.

XRD structures of **2** (left) and **5** (right). Ellipsoids shown at 50% probability. Selected bond distances (Å): **2**, Fe1-H1 = 1.42(2), Fe1-H2 = 1.49(2), B1-H2 = 1.17(2), Fe1-B1 = 2.604(3); **5**, Fe1-H42 = 1.35(2), Fe1-H43 = 1.52(2), B1-H43 = 1.20(2), Fe1-B1 = 2.673(2).

NIH-PA Author Manuscript

NIH-PA Author Manuscript

NIH-PA Author Manuscript

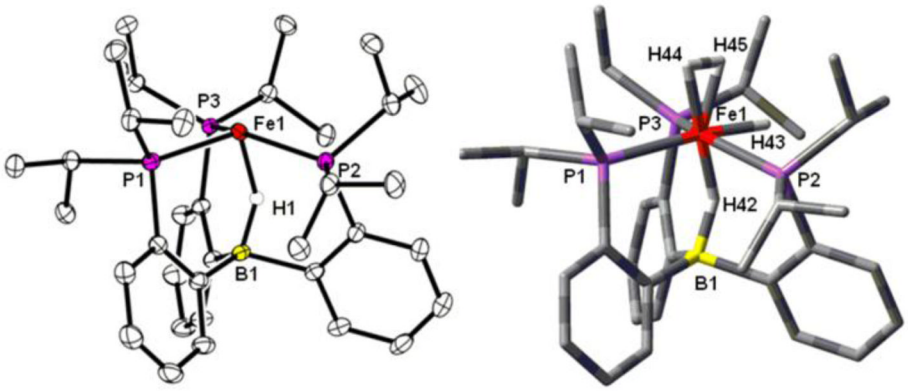

Figure 2.

XRD (left) and DFT optimized (right) structures of **3**. Ellipsoids shown at 50% probability. Selected bond distances (Å) and angles (°): XRD, Fe1-H42 = 1.56(2), B1-H42 = 1.21(2), Fe1-B1, 2.63(2), P2-Fe-P3 = 136.54(2); DFT predicted, Fe1-H42 = 1.51, Fe1-H43 = 1.50, Fe1-H44 = 1.62, Fe1-H45 = 1.59, B1-H42 = 1.24, Fe1-B1 = 2.63, H44-H45 = 0.84, P2-Fe1-P3 = 140.63.

NIH-PA Author Manuscript

NIH-PA Author Manuscript

NIH-PA Author Manuscript

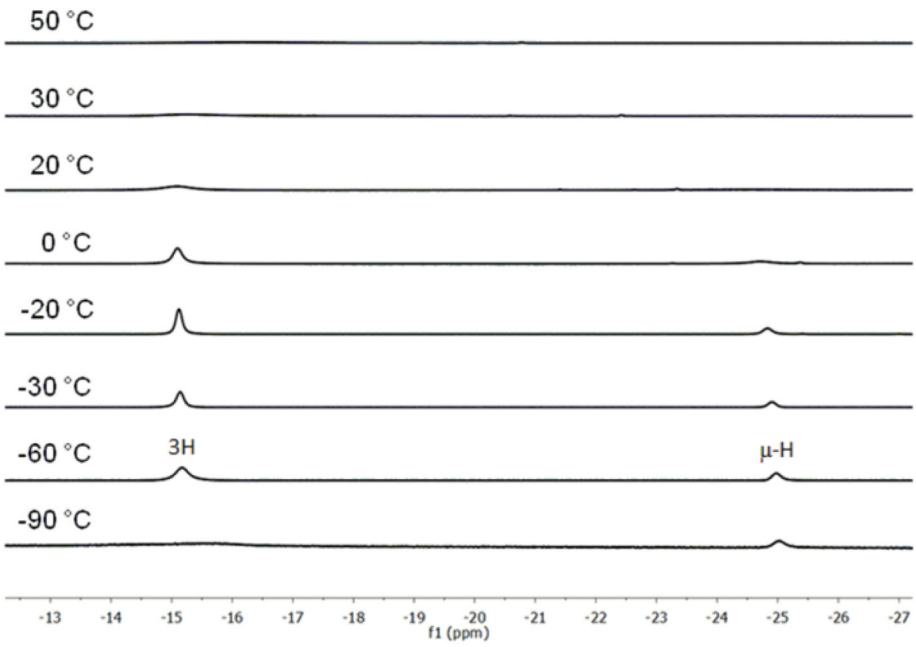

Figure 3.
^{1}H VT-NMR spectra of **3** in d_8-toluene under 1 atm of H_2.

NIH-PA Author Manuscript

NIH-PA Author Manuscript

NIH-PA Author Manuscript

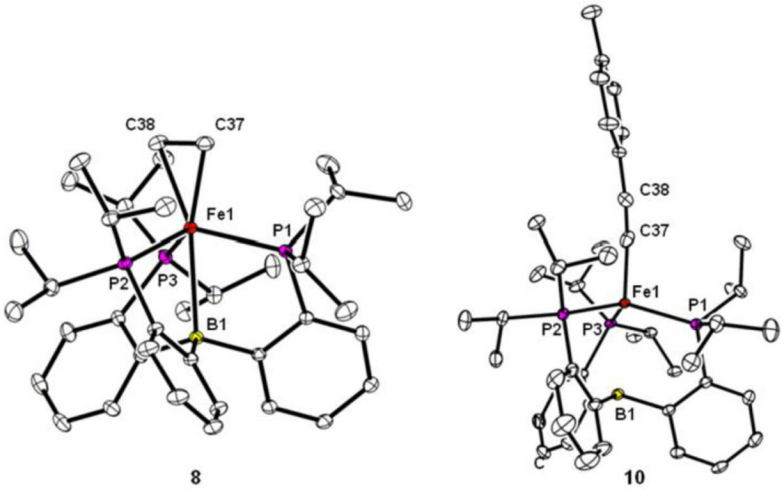

Figure 4.

XRD structures of **8** (left) and **10** (right). Ellipsoids shown at 50% probability. Selected bond distances (Å) and angles (°): **8** (average for two molecules in the asymmetric unit cell), Fe1-B1 = 2.491(1), Fe1-C37 = 2.103(1), Fe1-C38 = 2.113(1), C37-C38 = 1.397(2), Σ(P-Fe-P) = 338.76(3); **10** (average for two molecules in the asymmetric unit cell), Fe1-B1 = 2.761(2), Fe1-C37 = 1.918(2) C37-C38 = 1.169(3), Σ(P-Fe-P) = 345.07(2).

NIH-PA Author Manuscript

NIH-PA Author Manuscript

NIH-PA Author Manuscript

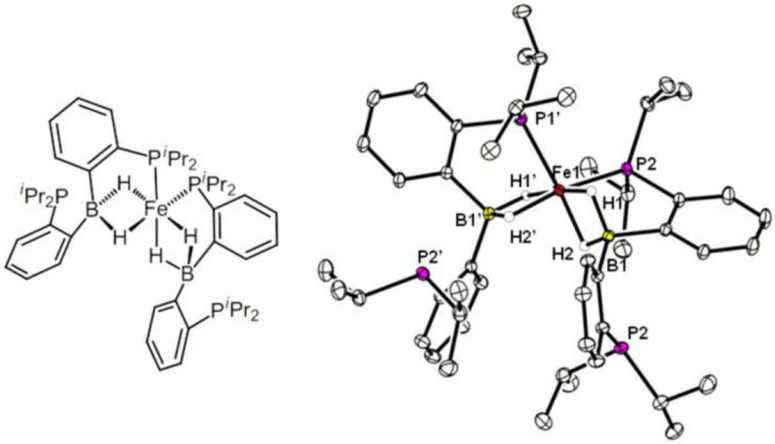

Figure 5.

Chemical line representation and XRD structure of **11**. Ellipsoids shown at 50% probability. Selected bond distances (Å): Fe1-H1 = 1.59(1), Fe1-H2 = 1.63(1), Fe1-B1 = 2.0900(6), Fe1-P1 = 2.2481(2).

NIH-PA Author Manuscript

NIH-PA Author Manuscript

NIH-PA Author Manuscript

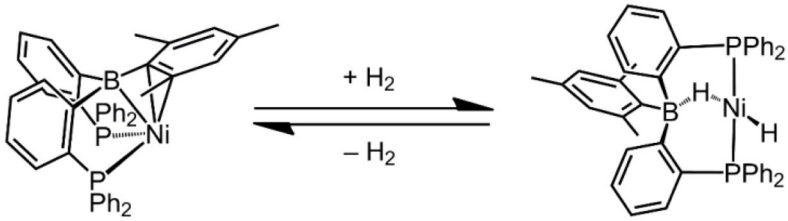

Scheme 1.
Related H_2 Activation Across a Ni-B Bond

NIH-PA Author Manuscript

NIH-PA Author Manuscript

NIH-PA Author Manuscript

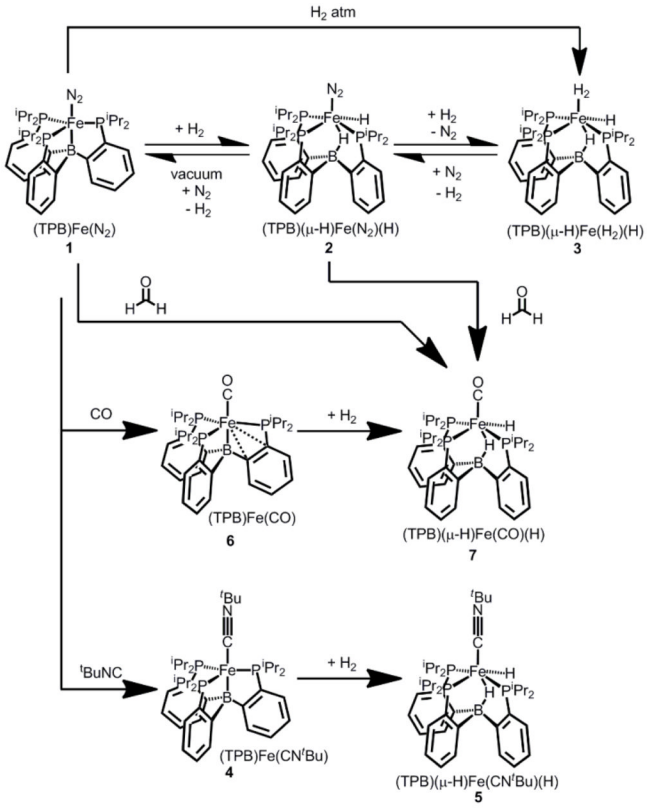

Scheme 2.
H-H and E-H Bond Activations Across Fe-B Bonds

NIH-PA Author Manuscript

NIH-PA Author Manuscript

NIH-PA Author Manuscript

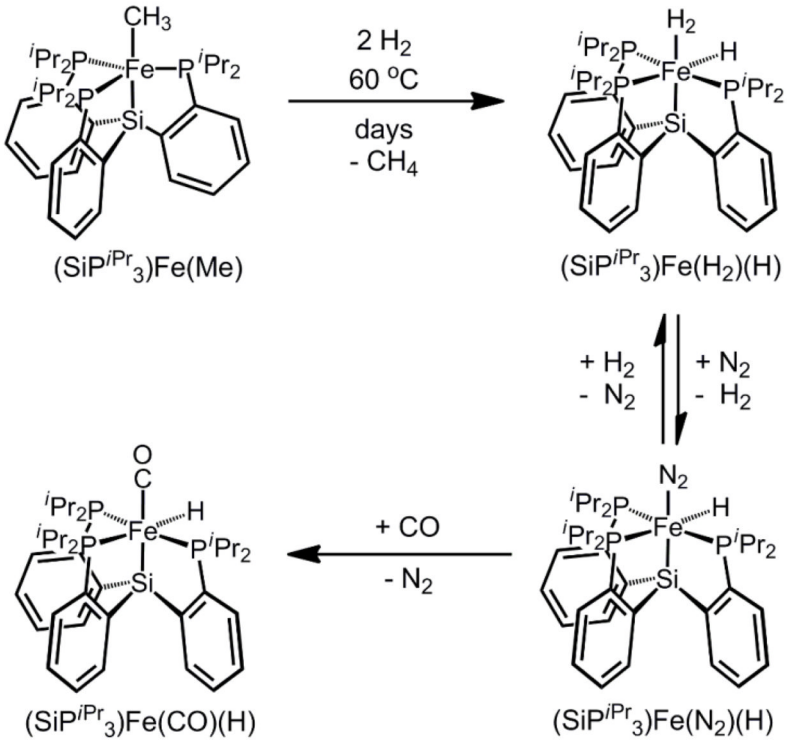

Scheme 3.
Chemistry of the Related Silatrane System

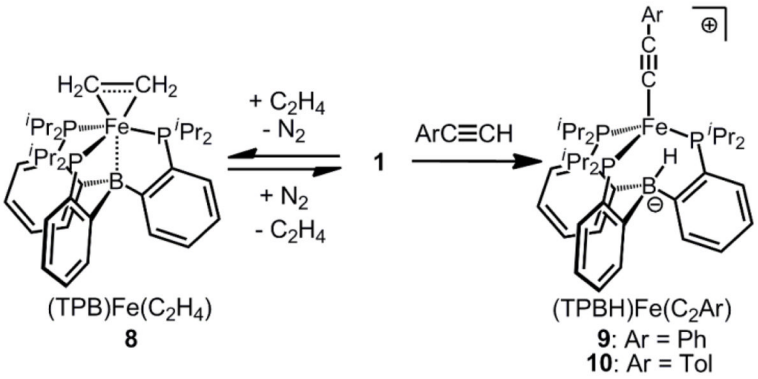

Scheme 4.

Ethylene Coordination and Arylacetylene C-H Bond Activation by **1**

NIH-PA Author Manuscript NIH-PA Author Manuscript NIH-PA Author Manuscript

NIH-PA Author Manuscript

NIH-PA Author Manuscript

NIH-PA Author Manuscript

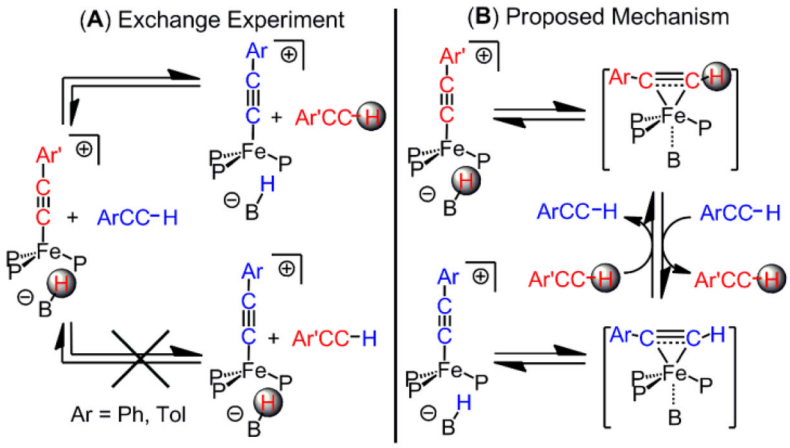

Scheme 5.
Reversible Arylacetylene C-H Bond Activation

NIH-PA Author Manuscript

NIH-PA Author Manuscript

NIH-PA Author Manuscript

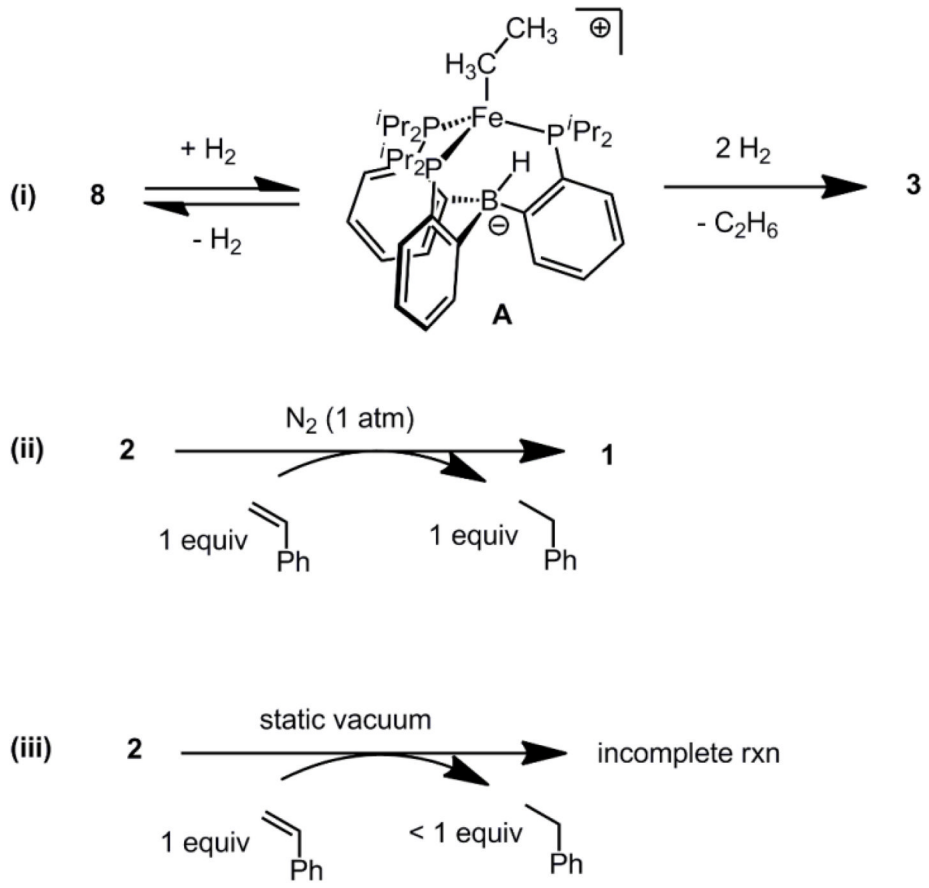

Scheme 6.
Stoichiometric Hydrogenation Reactions

NIH-PA Author Manuscript

NIH-PA Author Manuscript

NIH-PA Author Manuscript

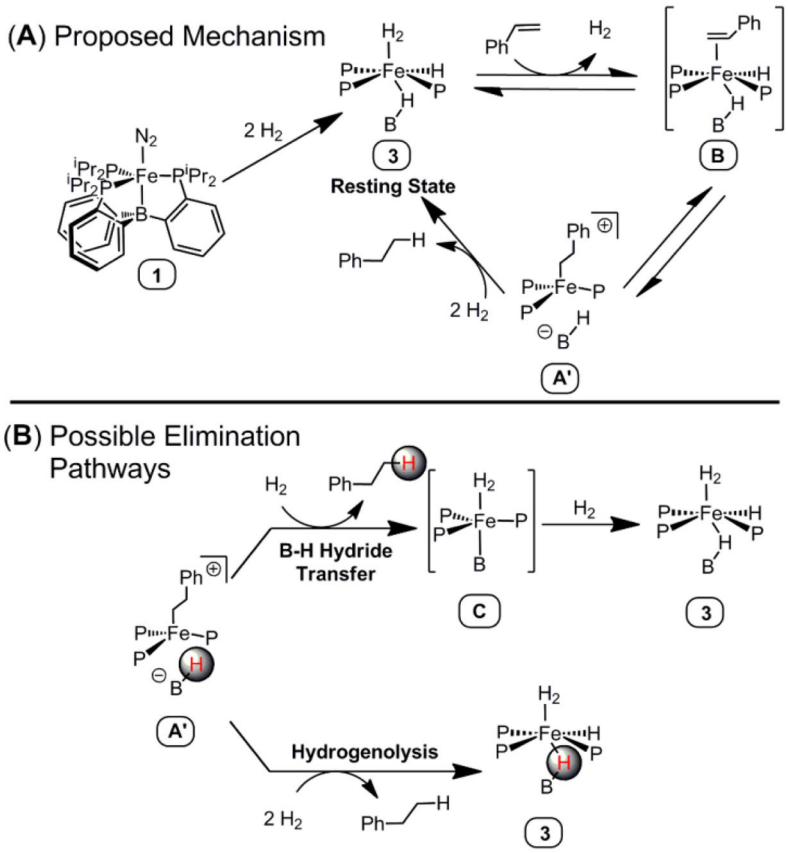

Scheme 7.
Mechanism and Alkane Elimination Pathways

NIH-PA Author Manuscript

NIH-PA Author Manuscript

NIH-PA Author Manuscript

Table 1

Catalytic Hydrogenations by **1** with H_2

Precatalyst	Substrate	Product	TOF (h^{-1})
1	Ethylene[a]	Ethane	15
1	Styrene[a]	Ethylbenzene	0.27
1	Phenylacetylene[b]	Ethylbenzene	0.16

Conditions: Room temperature, 0.01 M **1**, 1 atm H_2, and 0.01 M ferrocene as an internal integration standard in d_6-benzene.

[a]0.3 M substrate,

[b]0.29 M substrate.

[c]As determined by ^{1}H NMR spectroscopy at > 95% product.